Final Report for TWDB Contract No. 1004831025

Large woody debris in the lower San Antonio River

Final Report

J.K. Haschenburger
University of Texas at San Antonio

with assistance from

Benjamin Cardenas

and

Brandy Walker

June 1, 2012

CONTRACT ADMINISTRATION
2012 JUN 13 PM 2:50

Final Report for TWDB Contract No. 1004831025

Large woody debris in the lower San Antonio River

J.K. Haschenburger
University of Texas at San Antonio

with assistance from

Benjamin Cardenas

and

Brandy Walker

June 1, 2012

1 Introduction

Large woody debris (LWD) is a natural component along most rivers, influencing the function of the channel and the riparian ecosystem. LWD affects channel hydraulics (Manga and Kirchner, 2000) and changes sediment transfers through watersheds (Montgomery et al., 1996), which can affect channel stability and stream communities through the availability and quality of stream habitat (Hogan, 1987; Hyatt and Naiman, 2001; Keller and Swanson, 1979; Lemly and Hilderbrand, 2000). The purpose of this study was to investigate the amount and effect of large woody debris (LWD) in the lower San Antonio River by quantifying the wood loading and evaluating the effect LWD might have on bankfull discharge and channel stability. This report describes the study reach, the methods employed, and the results derived for each aspect of the study.

2 Study reach

The 7.4 mile long study reach extends from the US Geological Survey (USGS) streamflow gauging station (08188570 San Antonio River near McFaddin) located at State Highway 77 to Elm Bayou (Figure 1). The reach is entirely within the distributary network of the river's delta and the study is focused on the dominant channel identified as the San Antonio River. This channel has low sinuosity and is bordered mostly by agricultural landuse, although there are sections where a riparian forest exists.

2.1 Channel characteristics

In the study reach at the time of fieldwork, the flow width, determined by a range finder, was 123.6 ± 2.9 ft and mean depth, measured by a handheld depth sounder, was 12.5 ± 0.6 ft (Table 1). Sediment samples collected from the streambed using an Ekman sampler and banks using a trowel near the upstream and downstream limit of the study reach indicate that more than 70% of the sediment consists of sizes smaller than sand (Table 1).

3 Wood loading

3.1 Methods

Over most of the study reach, the wood loading was established by field survey. At the end of the study reach, aerial photography was used to estimate wood volume, given the presence of a jam that prevented boat access and the difficulty of accessing the entire length of the jam over land.

3.1.1 Field inventory

The field inventory was completed between June 25, 2010 and February 13, 2011. During this period, four floods occurred, three with a peak discharge of around 1000 ft^3s^{-1} on July 5 and 31 and January 20 and one with a peak of 8770 ft^3s^{-1} on September 14. As a result of these floods, some LWD already inventoried in the upper section of the study reach could have moved downstream into other sections that were subsequently surveyed.

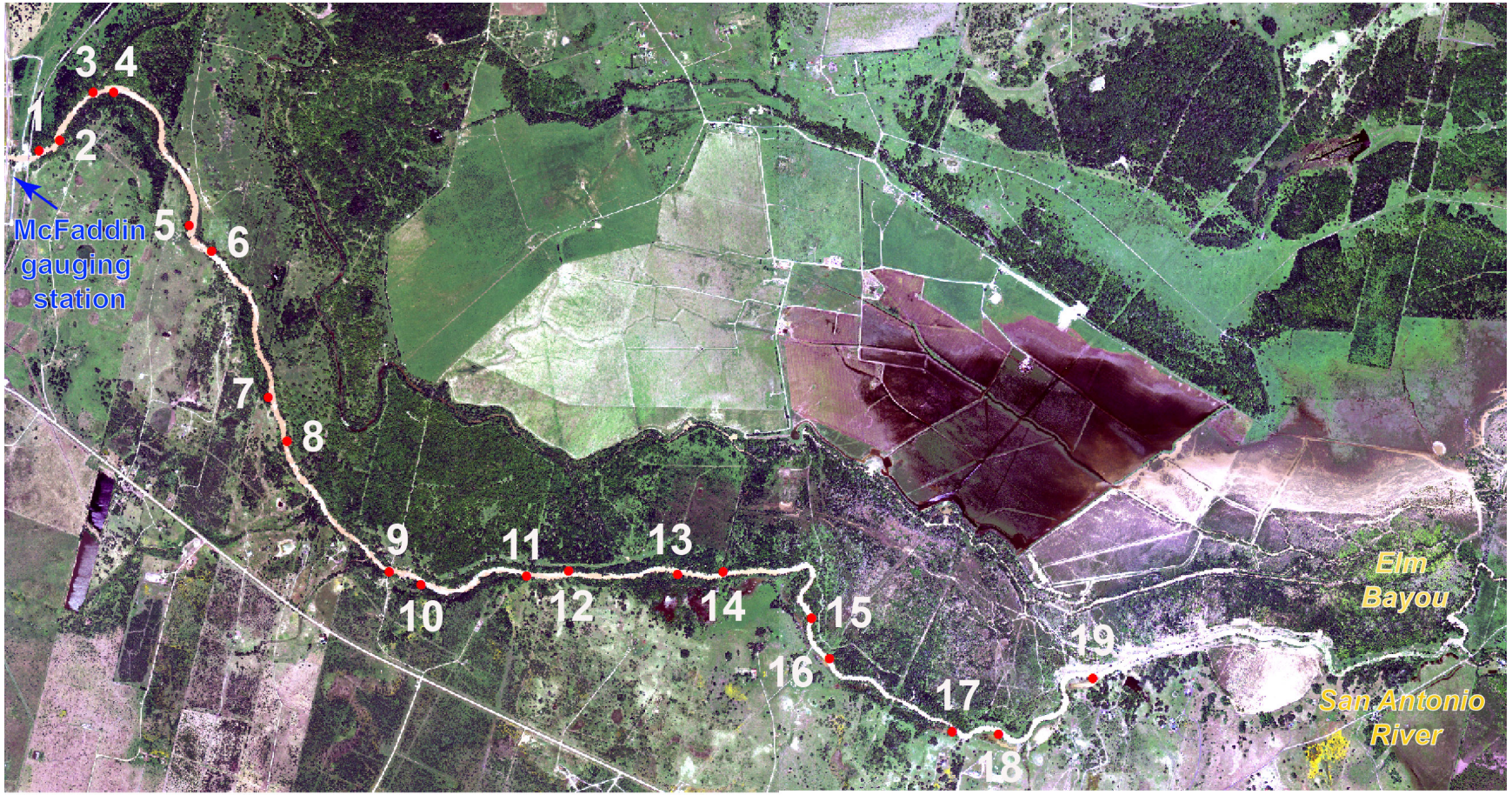

Figure 1. The lower reach of the San Antonio River. Flow direction is from left to right. Circles show the midpoint of subreaches used in the study except for the most downstream symbol that indicates the upstream limit of the last subreach. The far left boundary is defined by State Highway 77 where streamflow gauging station is located.

Table 1. Channel characteristics in the study reach

Sampling location	Subreach			Mean flow width[b] (ft)	Mean flow depth[b] (ft)	% <0.0025 in.	
	Number	Midpoint[a] (miles)	Length (ft)			Bed sediment	Bank sediment
1	1	0.14	230	116 ± 1	8.8 ±3.8	91.8	76.3
	2	0.23	230	130 ± 10	13.3 ±1.4		
2	3	0.44	230	128 ± 1	11.7 ±1.5		
	4	0.52	230	144 ± 2	9.1 ±2.9		
3	5	1.16	459	131 ± 2	11.2 ±3.9		
	6	1.30	459	138 ± 2	10.0 ±0.4		
4	7	1.90	459	141 ± 1	10.1 ±3.0		
	8	2.07	459	119 ± 1	11.2 ±1.1		
5	9	2.70	459	104± 3	18.1 ±4.4		
	10	2.83	459	115 ± 1	14.9 ±2.1		
6	11	3.24	459	112 ± 4	14.3 ±3.1		
	12	3.40	459	137 ± 2	15.4 ±2.1		
7	13	3.80	459	114 ± 5	15.4 ±2.9		
	14	3.97	459	119 ± 2	15.6 ±4.0		
8	15	4.51	459	109 ± 1	10.7 ±3.2		
	16	4.69	459	110 ± 2	10.8 ±2.5		
9	17	5.25	459	125 ± 1	11.7 ±2.1		
	18	5.43	459	133 ± 2	12.2 ±2.3	72.1	83.0
10	19	6.69	7930	c	c		

a From the Highway 77 bridge
b ± standard error
c Information not estimated from aerial photography

Subreaches inventoried for LWD were selected based on a stratified random sampling strategy with the first location established by randomly selecting a starting distance for the inventory. Two subreaches were inventoried for each sampling location so that local variability in wood loading could be assessed. The paired subreaches were 140 m in length in general (or about 4 times the wetted channel width) and separated by a comparable distance (Table 1). The paired subreaches were separated from each other by a mean interval of 2830 ft, which is approximately 6 times the subreach length. This strategy resulted in 23.4% of the boat accessible study reach being field inventoried.

In each subreach, the in-channel inventory included individual pieces of woody debris exposed along the channel boundary but not submerged pieces (Figure 2). Woody debris that was at least 3.3 ft long and 3.9 inches in diameter was included in the inventory based on previous studies (Hassan et al., 2005). Debris orientation relative to the flow channel and the presence of a root wad was noted to assess potential mobility of the debris.

Figure 2. Pieces of woody debris in the upper section of the study reach.

Based on the assumption of a perfect cylinder the volume of individually measured pieces of debris was determined as

$$V_i = \pi r_i^2 l_i \qquad [1]$$

where V_i = volume, r_i = radius, and l_i = length of the wood piece i. Based on field observations most wood conformed to the cylinder shape given the general absence of root wads.

Additionally, when woody debris was accumulated into small jams (Figure 3), pieces that met the minimum size criteria were inventoried individually but information was also collected on the spatial extent and mean diameter of the pieces comprising the jam in general. These accumulations consisted mostly of pieces smaller than the minimum size.

3.1.2 Photo Inventory

The spatial area of LWD downstream of the field inventoried reach was quantified by using ENVI, an image analysis software package. This strategy allowed for open water areas within the extended jam to be easily discerned and subtracted out for a wood volume estimate. Only a volumetric loading was attempted due to the difficulty of defining individual wood pieces from the photography. Additionally, debris smaller than the minimum size criteria is most likely included in the computed volume and therefore it is overestimated relative to the field inventoried volume. Orthophotography from 2011 was used because the date most closely corresponds to the timing of the field inventory.

Figure 3. LWD accumulation. Most pieces are smaller than the minimum size criteria employed

The image analysis was coupled with two field observations taken along the upstream boundary of the jam to permit an estimate of wood volume. First, the initial 3.3 ft length of the jam was divided into 9 sections that were 3.3 ft wide. At each section, two marked 3.3 ft long photograph scales were positioned at a 90° angle on top of the debris and then the area was photographed to determine the proportion of wood to open space. This analysis gave a wood proportion of 30 to 40% for a porosity estimate of 70 to 60%, respectively. Second, the measurement areas were subdivided into 9 subunits and a ruler was placed in the middle to probe for wood thickness. These observations produced a mean wood thickness of 0.64 ft. Field observations suggest that most debris pieces were floating at the water surface and therefore this thickness is a reasonable estimate based on the range of wood diameters derived from the field inventory (discussed below). Field observations of LWD characteristics did not appear to change significantly over the 1000 ft length inspected.

The wood volume of the extended jam in subreach 19 was computed as

$$V_j = A\, d\, (1\text{-}\Phi) \qquad [2]$$

where V_j = wood volume of the jam, A = spatial area of wood, d = wood thickness, and Φ = jam porosity. The volumetric estimate was assigned to the midpoint distance of the subreach. An estimate of delivery rates of LWD to the subreach was determined for two periods using this analysis strategy. Aerial photography taken on January 30, 2009 shows that the LWD present in 2008 was removed from the channel (Figure 6). This allowed accumulated volumes to be estimated for two time periods based on subsequent aerial photographs taken on April 24, 2010 and March 10, 2011. However, the 2010 volume may be underestimated because of the poor color quality of the photography and the higher discharge at the time, which may have submerged some of the LWD.

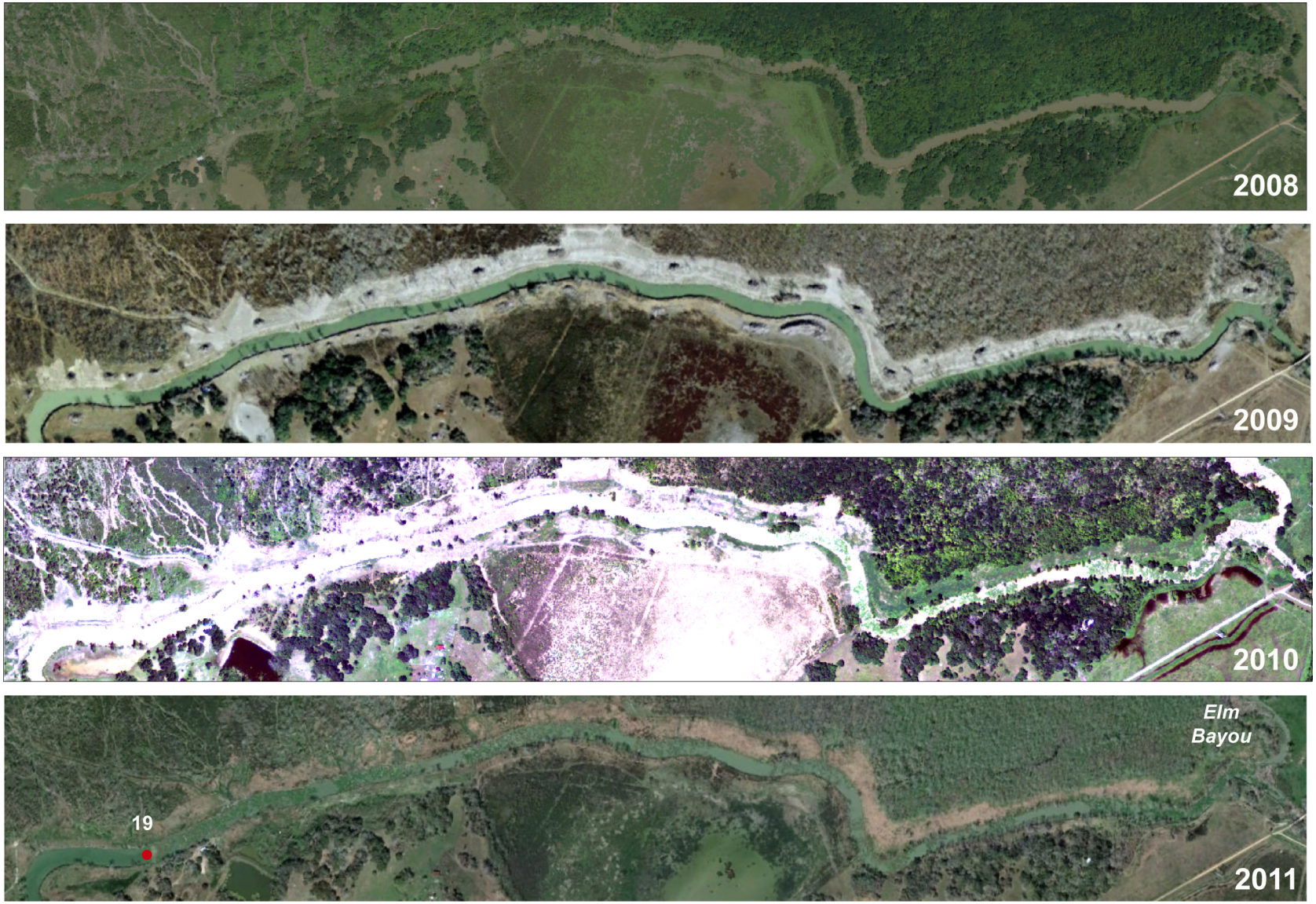

Figure 6. Accumulation of large woody debris in subreach 19. Flow direction is from left to right. The upstream limit of the subreach is indicated by numbered circle on the 2011 image.

3.2 Results

The total number of woody pieces inventoried was 371 over the 1.4 miles of the subreaches (Table 2). Based on the standard metrics advocated by Wohl et al. (2010), the wood loading is 16.6 pieces per 100 m of channel for the inventoried reach. This loading is relatively small compared to rivers in the Pacific Northwest (e.g., Benda et al., 2002; Hassan et al., 2005) but exceeds loadings in the nearby Sabine River, which range from 2.9/100 m to 11.2/100 m (McBroom, 2010).

The number of wood pieces varies between subreaches, ranging from 2.1 to 80 pieces per 100 m (Table 2), and documents that LWD is not evenly distributed along the study reach (Figure 4). Nonetheless, the paired Wilcoxon statistic indicates that there is no statistical difference between subreach values (p-value = 0.91, $\alpha = 0.05$). The highest concentration occurs in the first three subreaches, which may reflect the influence of the three bridges upstream, and between river miles 2.8 and 4.0. In general, most of the debris was found near the interface between the wetted channel and banks (Figure 2). In some cases, wood was floating on the upstream side of fallen trees or debris protruding from the bank into the wetted channel. Most pieces were oriented orthogonal to the flow channel (52%), followed by a parallel position (38%). Thus, only about half of the debris, if immobile, has the maximum potential to locally affect channel stability through obstruction scour.

Table 2. LWD characteristics and loading

Subreach	Subreach midpoint[a] (miles)	Number of pieces	Pieces /100 m	Mean length[b] (ft)	Mean diameter[b] (in.)	Wood volume (ft^3)	Unit volume (m^3/100 m)
1	0.14	42	60.0	12.2 ±1.7	8.8 ±0.8	229	9.3
2	0.23	54	77.1	11.3 ±1.2	8.5 ±0.6	103	4.2
3	0.44	56	80.0	10.1 ±1.3	8.4 ±0.8	262	10.6
4	0.52	14	20.0	11.8 ±2.6	11.1 ±2.3	196	7.9
5	1.16	7	5.0	10.0 ±2.3	9.5 ±1.8	57	1.1
6	1.30	33	23.6	12.6 ±1.7	8.6 ±1.0	376	7.6
7	1.90	4	2.9	5.7 ±0.6	4.7 ±0.6	3	0.1
8	2.07	9	6.4	11.5 ±3.0	8.5 ±1.6	95	1.9
9	2.70	9	6.4	11.6 ±1.7	6.8 ±0.9	33	0.7
10	2.83	33	23.6	12.4 ±1.2	9.4 ±0.8	242	4.9
11	3.24	21	15.0	12.7 ±0.8	10.6 ±1.6	257	5.2
12	3.40	14	10.0	14.4 ±2.1	9.3 ±1.3	169	3.4
13	3.80	41	29.3	12.9 ±1.1	8.4 ±0.8	436	8.8
14	3.97	18	12.9	12.4 ±1.2	8.0 ±0.7	91	1.8
15	4.51	4	2.9	17.2 ±3.6	11.9 ±1.5	52	1.1
16	4.69	3	2.1	9.3 ±1.4	8.9 ±4.4	14	0.3
17	5.25	6	4.3	12.5 ±0.2	6.8 ± 0.1	22	0.4
18	5.43	3	2.1	12.0 ±4.8	11.2 ±2.9	18	0.4
19	6.65	c		c	c	69676	81.6

a Downstream from the Highway 77 bridge

b ± standard error

c Information not estimated from aerial photography

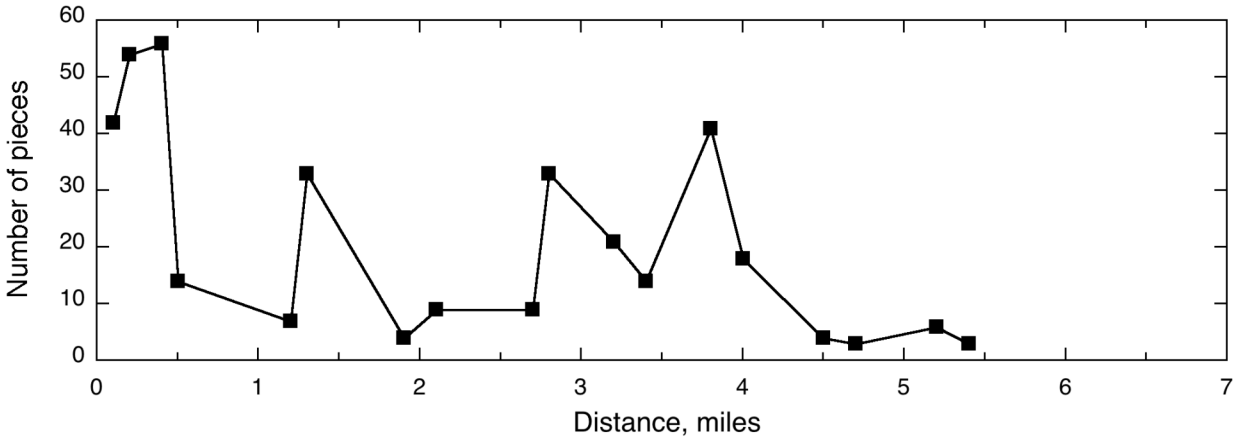

Figure 4. Number of LWD pieces as a function of distance

Individual pieces averaged 11.9 ± 0.4 ft long and 8.8 ± 0.3 inches in diameter (Table 2), giving an average volume for a piece of debris of 3.2 ± 0.4 ft^3. Very large pieces of woody debris are rare. The mean length is only 32% of the wetted channel width, indicating the potential for high mobility in general. Further, only about 5% of the inventoried pieces had root wads, suggesting that log mobility is not significantly inhibited by this mechanism. Based on these indicators, the LWD has high potential for mobility except where riparian vegetation effectively traps debris.

Of the 371 inventoried pieces, 33% were associated with accumulations of woody debris, where most pieces were smaller than the minimum size criteria. These accumulations are typically one log diameter high and very loosely packed. On an areal basis, these accumulations amount to 4615 ft^2 and cover <1% of the channel area inventoried (Table 3). Given the greater mobility of the smaller pieces, the size of these jams would be expected to be fairly transient, changing in response to floods that remove and add pieces.

For the field inventoried reach, the total wood volume of 2655 ft^3 translates into 1907 ft^3 per mile of channel. Subreach volumes range from 3 ft^3 to 436 ft^3 (Table 2, Figure 5) with paired subreaches differing by up to 231 ft^3, which highlights the local variability in wood storage in this low sinuosity channel. Nonetheless, the paired Wilcoxon statistic indicates that there is no statistical difference between subreach values (p-value = 0.65, $\alpha = 0.05$). On a per unit length basis, the wood volume converts to 3.4 m^3/100 m for the field inventoried reach. Including subreach 19 with the extended jam increases the total volume to 21,237 ft^3 or a loading of 82 m^3/100 m. The volumetric loading falls within the lower range of LWD studies conducted in the Pacific Northwest. Compared to the nearby Sabine River, where the volumetric loading ranges from 0.6 to 8.5 m^3/100 m, the lower San Antonio stores a comparable amount in the field inventoried reach but has substantially more debris when the extended jam is included.

Observations of the transport of LWD during floods upstream at Goliad suggest that it occurs in an uncongested mode (Braudrick et al., 1997) and, based on the ratio between average wood size and baseflow width, is easily transported toward the Elm Bayou confluence. Based on aerial photography, LWD tends to accumulate at the confluence and in the reach upstream of it (Figure 6). The rate of LWD delivery to subreach 19 is estimated at 31,412 ft^3yr^{-1} for the period between

Table 3. Characteristics of field inventoried jams

Reach	Jam dimensions (ft)	Mean log diameter (in.)	Coverage area (ft^2)
1	45.3 x 11.5	7.9	520
	9.8 x 3.3	3.9	32
	6.6 x 6.6	7.9	43
2	9.5 x 8.3	5.9	79
	27.0 x 12.0	9.8	324
	24.0 x 11.0	3.9	264
	7.0 x 7.0	13.8	49
3	7.0 x 12.0	3.9	84
	43.6 x 13.1	9.8	573
	7.9 x 7.3	0.0	58
	9.8 x 3.3	5.9	32
6	6.0 x 10.0	3.9	160
	9.5 x 6.6	3.9	62
	23.3 x 8.9	3.9	206
9	18.0 x 17.1	3.9	308
10	15.7 x 12.0	7.9	188
	39.4 x 13.1	9.8	517
13	41.7 x 22.6	13.8	943
14	13.1 x 13.1	9.8	172

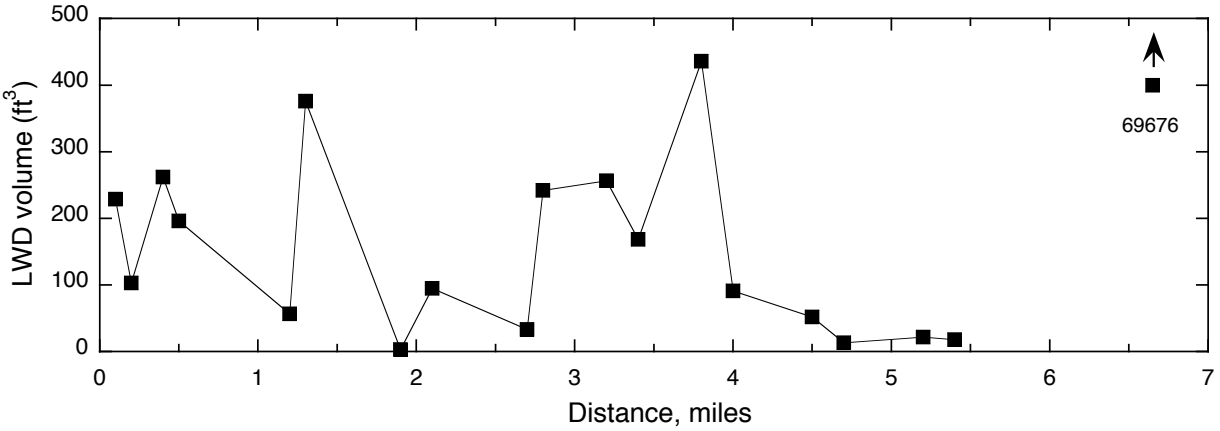

Figure 5. LWD volume as a function of distance

January 30, 2009 and April 24, 2010, and 35,449 ft^3yr^{-1} for the period between April 24, 2010 and March 10, 2011. In both periods, mean daily discharge exceeded 7000 ft^3s^{-1} (exceedence probability of 1.5%), with the number of days equaling 5 and 3 for the two periods, respectively. The confluence effectively reduces the likelihood of debris transport because flow is divided

between the two channels, reducing flow depth (Bilby and Ward, 1989). The confluence also changes the local sinuosity of the channel, which facilitates deposition of debris (Lienkaemper and Swanson, 1987). Further, the complex distributary network along the main channel, particularly noticeable on the north side, helps direct higher flows across the surrounding wetland and thereby reduces debris mobility by limiting the maximum flow depth in the channel.

4 Effect on bankfull discharge

4.1 Methods

The effect LWD loading might have on the discharge causing overbank flow was evaluated by establishing bankfull flow conditions at the McFaddin gauge and then systematically adjusting the available flow area by different amounts of LWD to determine the discharge at bankfull capacity and its exceedence probability. First, a discharge-stage relation was established to estimate the bankfull discharge at the USGS-delineated bankfull stage of 29.0 ft (Figure 7) using discharge measurements collected by the USGS to maintain the station's rating curve. Of the 56 measurements, two exceed the bankfull stage but only data from the smallest overbank flow were used because the larger flow showed sharp departures in mean flow depth and velocity as would be expected with significant overbank flow. A second-order polynomial function provided the best fit at relatively high discharges (Figure 7).

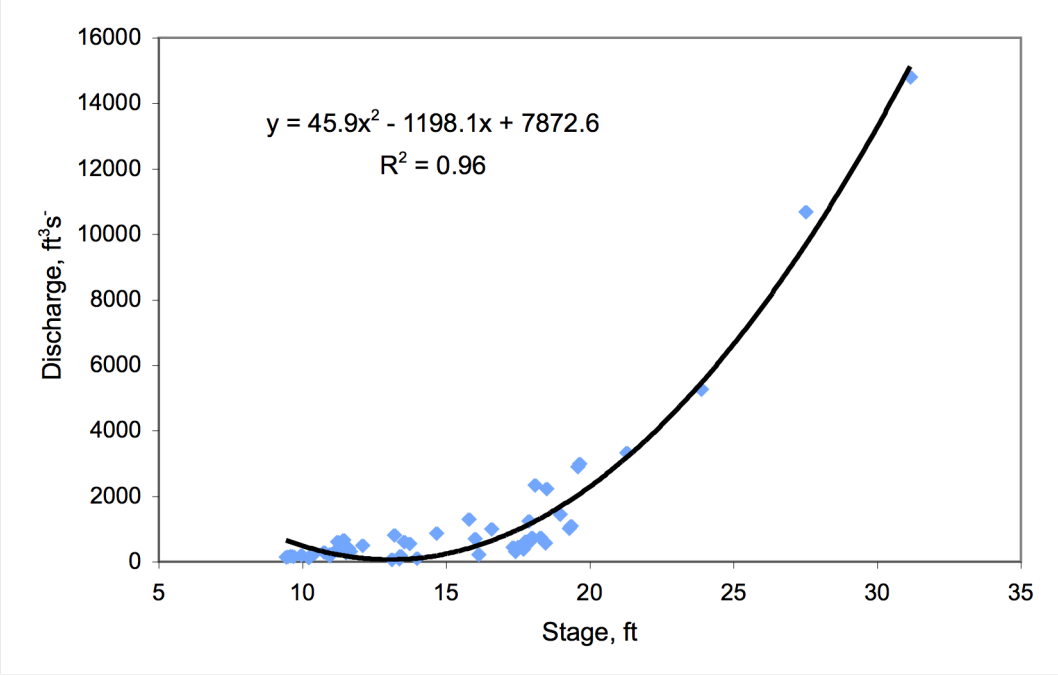

Figure 7. Discharge-stage rating relation.

Second, using the same data set, flow dimensions at bankfull discharge were estimated from relations of flow area and flow width with discharge (Figures 8 and 9). Third-order polynomial functions provided the best fit to the data. While departing from typically power functions, these polynomial functions provide a far superior fit. Additionally, the flow width at a baseflow

condition of 250 ft^3s^{-1} was computed to estimate a mean flow width for flows contained within the channel.

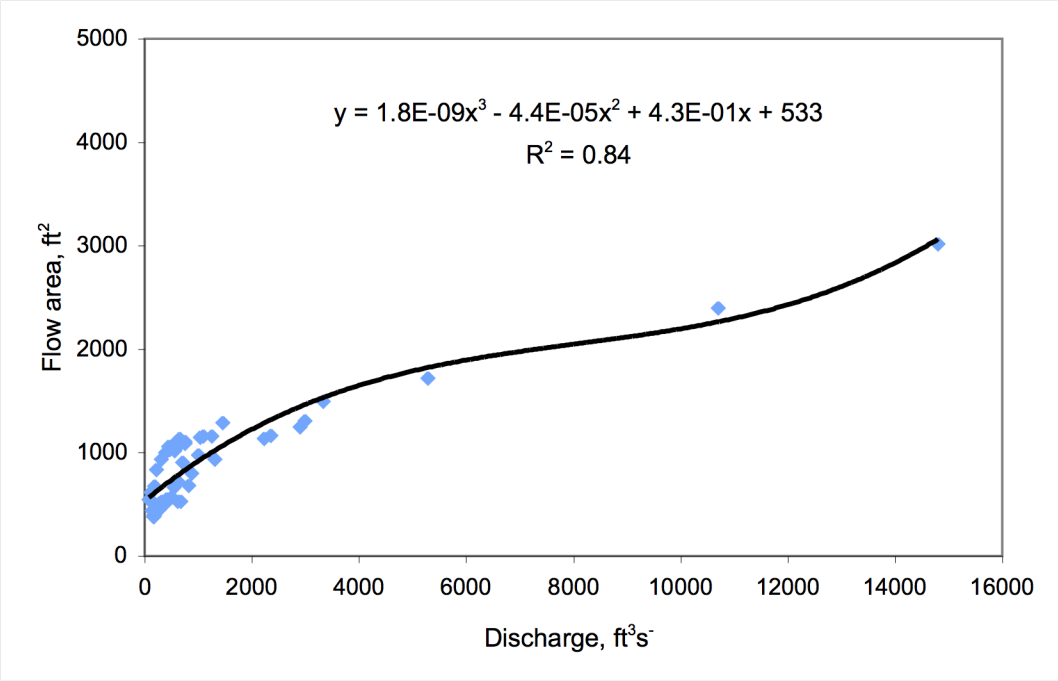

Figure 8. Relation between flow area and discharge

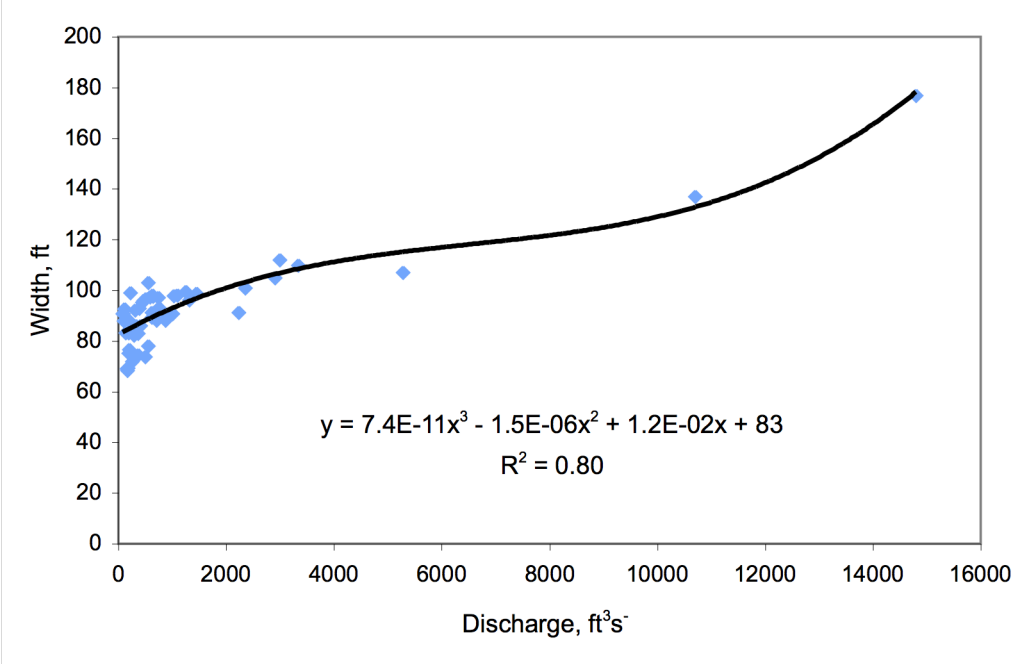

Figure 9. Relation between flow width and discharge

Woody debris was added to the channel cross section in layers, where the layer thickness was equal to the mean diameter of inventoried wood pieces. Each layer was assumed to extend a width equal to the mean channel flow width of 113 ft. This area was then adjusted to account for likely porosity with the value initially set equal to 65%, which is the estimate for the extended jam in subreach 19. A second scenario assumed tighter packing of debris and used a porosity of 45%. This adjusted wood area was then subtracted from the bankfull area of 2399 ft^2 and the associated discharge derived from an established relation between discharge and flow area (Figure 10). The exceedence probability for the adjusted discharge was then determined from the flow duration curve developed from all available streamflow data (Figure 11).

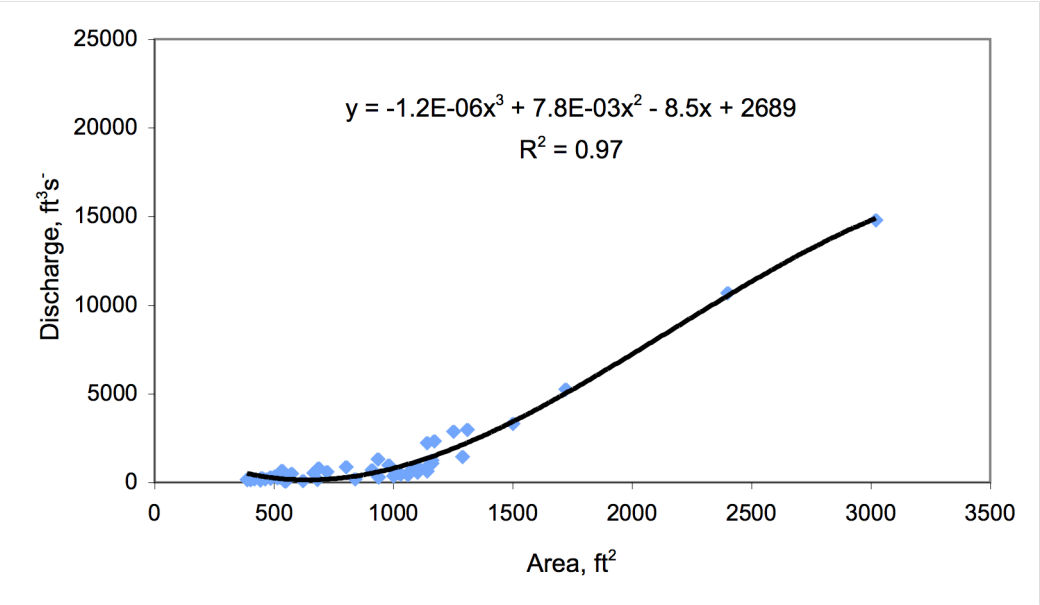

Figure 10. Relation between discharge and flow area

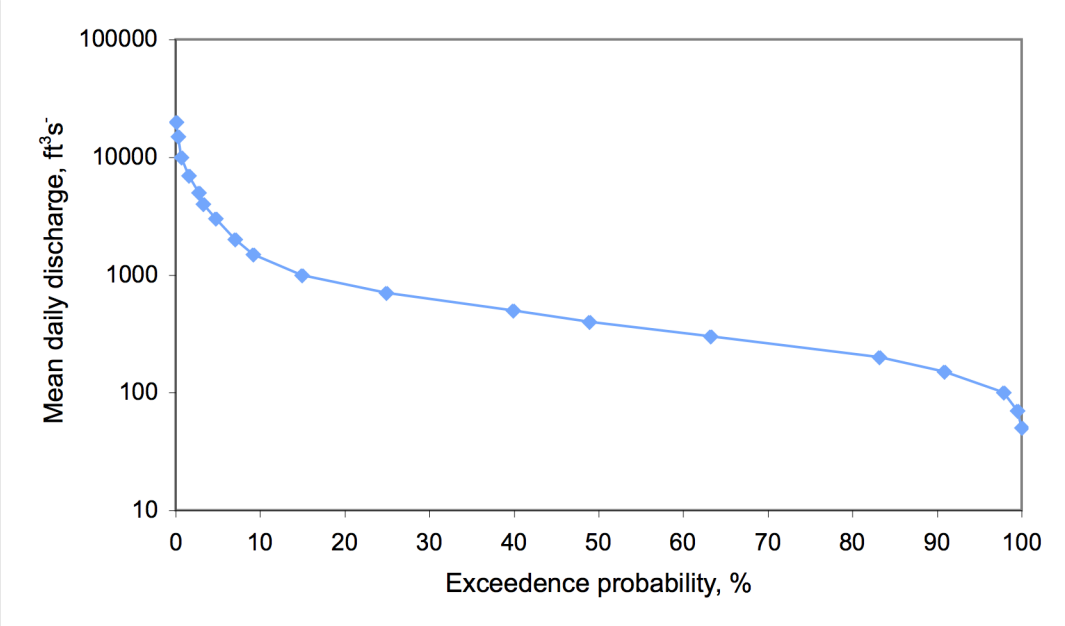

Figure 11. Flow duration curve for the McFaddin gauge.

4.2 Results

The bankfull discharge of 11,760 ft^3s^{-1} is exceeded 0.55% of the time. Assuming a jam porosity of 65%, bankfull discharge decreases from 9154 ft^3s^{-1} to 5088 ft^3s^{-1} as the proportion of debris increases from 20% to 80% (Table 4). This increases the likelihood of exceeding these discharges from 0.9 to 2.7%, and therefore the number of overbank floods. If the debris is more tightly packed, bankfull discharge decreases from 8362 ft^3s^{-1} to 2460 ft^3s^{-1}, which increases the exceedence probability from 1.1 to 5.9%, respectively.

Table 4. Bankfull discharge adjustments based on amount of LWD

LWD in cross section (%)	Jam porosity = 65%		Jam porosity = 45%	
	Bankfull discharge (ft^3s^{-1})	Exceedence probability	Bankfull discharge (ft^3s^{-1})	Exceedence probability
0	11770	0.55	11770	0.55
20	9154	0.92	8362	1.1
40	7769	1.3	6211	2.0
60	6403	1.9	4200	3.2
80	5088	2.7	2460	5.9

These estimates are a first approximation for at least three reasons. First, the results correspond to the area near the McFaddin gauge. The distributaries along the study reach would change the amount of discharge in the main channel, which may increase or decrease the exceedence probability depending on whether flow is being added or diverted. Any changes in bank height would also affect channel capacity and therefore the likely bankfull discharge. While LiDAR data suggest that the channel banks do not change radically along the reach, casual observations in the field suggest that banks are somewhat lower downstream of subreach 15. Second, the role of LWD in reducing flow velocity has not been incorporated. As a resistance element LWD would reduce flow velocity and increase flow depth for a given discharge. Therefore, the exceedence probabilities are most likely underestimated. Third, the estimates assume that the debris is immobile. General indicators of mobility suggest that debris should be relatively mobile and the adjustments to bankfull discharge may not materialize. In the extended jam, debris conditions at the upstream boundary suggest that at least some of the debris would float on the water surface as flood water rises rather than form a fixed obstacle within the bankfull channel. In fact, the visibility of LWD in the 2010 photography, when the discharge was 1150 ft^3s^{-1} supports this speculation (Figure 6). However, increased jam integrity through continued accumulation would increase the likelihood of LWD occupying fixed areas within the channel and exerting an effect on the channel and its flood regime.

5 Channel instability

5.1 Methods

Aerial photography was acquired electronically through the USGS Earth Explorer website and from the Texas National Resource Information System (TNRIS) (Table 5). Analysis procedures were standardized based on their effectiveness at the lowest scan resolution to minimize any impact from working with different scanning resolutions (Micheli and Kirchner, 2002; Mount et al., 2003; Tiegs and Pohl, 2005). Selected photography provides information about the river channel on an approximate 10-year interval, while utilizing the largest scale photography available.

Table 5. Aerial photography details

Acquisition Date	Frames	Scale	Color[b]	Agency	Discharge[c] (ft^3s^{-1})
11/1/1951[a]	2	1:17000	B&W	USGS	161
10/1/1959	4	1:21000	B&W	USGS	302
3/31/1966	4	1:20000	B&W	ASCS[d]	493[e]
11/11/1979	1	1:65380	CIR	NASA-AMES	337
10/12/1987	3	1:24000	B&W	TxDOT[d]	453
1/14/1995	8	1:40000	CIR	USDA-FSA (TOP96)[f]	468
4/24/2010	8	1:24000	RGBIR	USDA-FSA (NAIP2010)[f]	1110

a Partial coverage of study reach
b B&W = black and white; CIR = color infrared; RGBIR = RGB color infrared
c Based on Goliad gauge; 2010 value at McFaddin gauge = 1150 ft^3s^{-1}
d Acquired through TNRIS
e Average discharge based on two flight dates of 3/31/66 and 9/23/66
f Images georeferenced by source agency

Images were imported into ArcGIS for analysis. Except for 1995 and 2010 all photography required georeferencing. The 2010 photography was considered to have no spatial error and was used as a basemap to georeference the other photography. Georeferencing followed a two step procedure. First, each photograph was pinned to the 2010 photography with eight control points. One control point was placed near each corner and one point was placed halfway between each corner. If any point had a root mean square (RMS) an order of magnitude larger than the others, it was redone or replaced. Trees, road intersections, structures, and other persistent features were used as control points. Second, at least 12 control points were placed around the channel, which were distributed as evenly as possible on the north and south sides. However, the northern area had fewer persistent features and ultimately had fewer control points in every photograph. Rhoades et al. (2009) added control points until the RMS of the image was less than 3.3 ft. In this analysis, persistent features proved to be a limiting factor on the number of control points used and the image RMS that was achieved (Table 6).

Rhoades et al. (2009) argued that quadratic transformations can account for photographic distortions caused by the curvature of the Earth and used a second-order polynomial

transformation to georeference aerial photography. For San Antonio River, sensitivity analysis indicated that a third-order polynomial transformation produced images with less overall error on average, improving positional error by 2 ft and reducing the RMS by 9 ft (Table 6).

Table 6. Mean positional and RMS errors based on order of transformations

Year	Frame	2nd Order Error (ft)	2nd Order RMS (ft)	3rd Order Error (ft)	3rd Order RMS (ft)
1951	1	29.8	14.7	24.5	9.3
1959	1	23.2	23.2	12.7	8.2
	2	17.4	19.9	12.8	9.7
1966	1	16.6	10.7	16.5	5.9
	2	7.6	8.8	13.7	5.5
	3	8.6	11.0	16.0	6.4
	4	10.6	10.0	13.9	6.1
1979	1	24.6	30.2	13.2	11.5
1987	1	8.9	9.8	8.1	5.2
	2	9.0	9.6	6.2	5.8
	3	6.2	8.1	12.6	6.1

Channel position was defined by identifying the top of banks and then digitizing a centerline for each year of photography. Over some sections of the study reach, banks are obscured by a tree canopy. On the north and south sides the length amounts to 50% and 41% of the total study reach, respectively. Fortunately, frequent gaps exist where the bank is visible and the distance the canopy extends over the channel can be measured. Banks were identified with the assumption that this distance is locally constant (Gurnell, 1997). Using a fixed scale of 1:5000 (Yao et al., 2011), vertices of the centerline were digitized at a fixed interval for consistency (Mount et al., 2003). The 82 ft interval employed is slightly smaller than the average width of the wetted channel at baseflow to ensure that changes in the channel position were captured. Digitization was completed by a single operator to avoid inconsistencies that can occur with multiple operators (Tiegs and Pohl, 2005; Yao et al., 2011).

The eroded area polygon method (Micheli and Kirchner, 2002; Rhoades et al., 2009) was used to determine channel migration rates for each time interval and the entire study period. An eroded area polygon is created when two centerlines from two different images cross in two locations to define an area. Half of the perimeter of the defined area gives an mean stream length for the area, and the mean distance migrated equals the area of the polygon divided by this mean stream length. Rates of migration were calculated by dividing the mean migration distance by the time interval between a given pair of images. Only channel lengths that migrated beyond the mean positional error of 16 ft were considered to take into account most of the error associated with georeferencing (Rhoades et al., 2009).

5.2 Results

The migration rate for the channel over the study period is only 0.074 ft yr^{-1}, indicating that the position of the channel has been stable in terms of lateral position (Figure 12). Further, the migration rates for the 6 periods are fairly consistent, ranging from 0.082 ft yr^{-1} to 0.16 ft yr^{-1}. Sections where lateral shifting occurs exhibit migration rates that are up to two orders of magnitude larger than that for the entire study period (Table 7). However, these active sections make up only a small proportion of the channel length in any given period, which may be generally attributed to cohesive bank material and a low river gradient.

Table 7. Channel migration rates

Time period	Year interval	Number of years	Length of study reach (ft)	Channel length with lateral activity[a] (ft)	Mean migration rate over active sections[a] (ft yr^{-1})	Mean migration rate over study reach[b] (ft yr^{-1})
Study period	1951-2010	58.5	24957	8939	0.21 ± 0.03	0.074
Period 1	1951-1959	7.9	24957	5409	0.72 ± 0.11	0.16
Period 2	1959-1966	7.0	40236	2743	1.20 ± 0.33	0.082
Period 3	1966-1979	13.1	40236	10154	0.64 ± 0.08	0.16
Period 4	1979-1987	7.9	40236	7410	0.73 ± 0.10	0.14
Period 5	1987-1995	7.3	40236	6543	0.72 ± 0.12	0.12
Period 6	1995-2010	15.3	40236	6290	0.64 ± 0.18	0.10

a Exceeding error margin
b Calculated as a weighted mean of active and non-active reach lengths

A closer inspection of the reach upstream of the Elm Bayou confluence (i.e., subreach 19) indicates that no major change in channel position occurred over the study period. During the study period, the migration rate in this subreach is comparable to that in the study reach located upstream (Table 8). Between 1995 and 2010, the active migration rates are essentially identical but when the rate over the entirety of each reach is considered, lateral activity is actually less in subreach 19 (Table 8). Overall there is no significant difference between migration rates for the six time periods (Wilcoxon-Mann-Whitney statistic, p-value = 0.22 for active sections, p-value = 0.21 for reach, $\alpha = 0.05$). Nonetheless, in 2005 photography, there is evidence of LWD blocking the main channel, which forced more flow into the Elm Bayou channel. Removal of LWD in 2009 complicates any firm elimination of possible effects of a large amount of LWD. It may be that a measurable effect will occur only with longevity of the debris, particularly given the bank materials that would resist channel adjustment. With continued accumulation of LWD from upstream sources, the integrity of the jam would presumably increase (Hogan, 1987) and therefore the likelihood of adjustment to the channel.

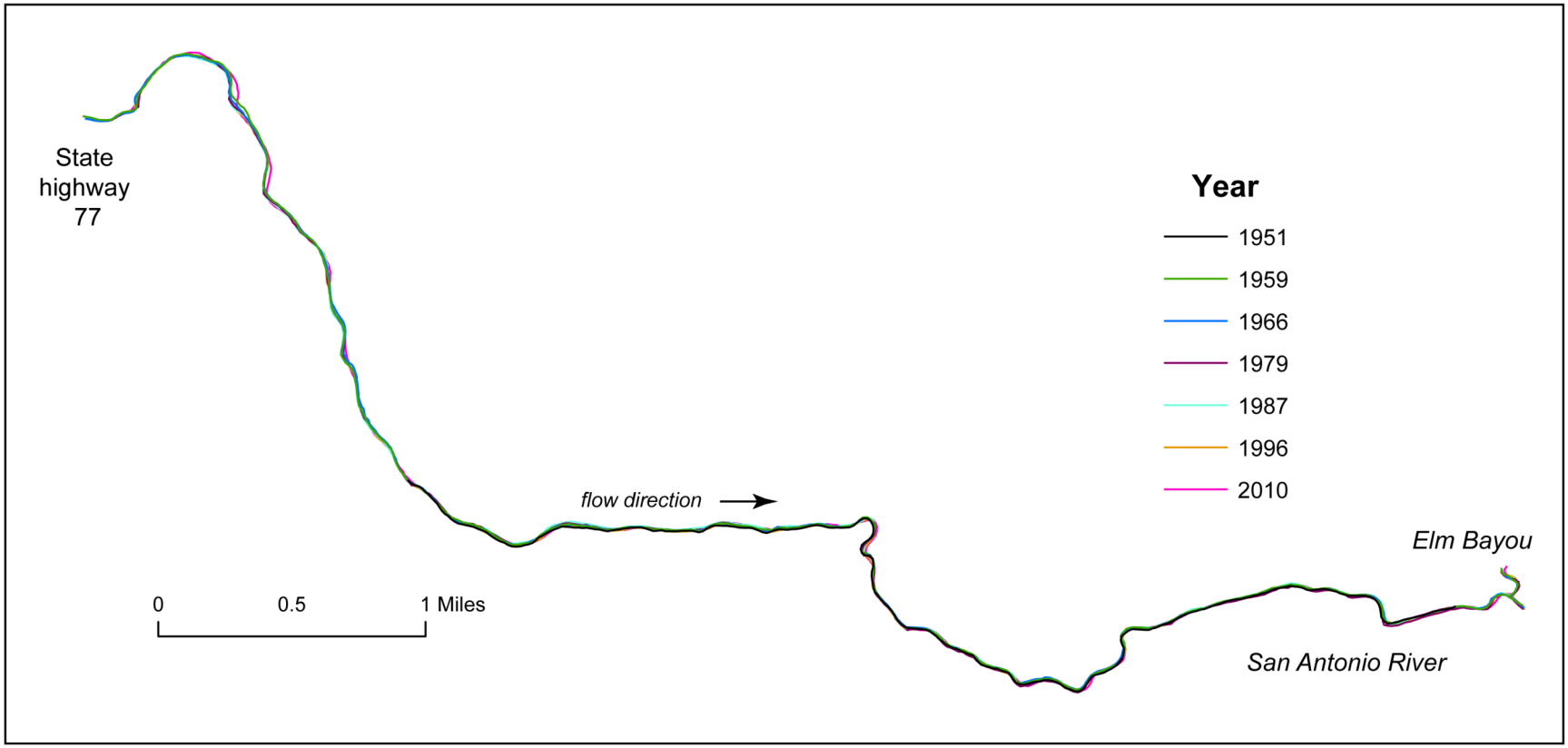

Figure 12. Channel position over time.

Table 8. Channel migration rates of subreach 19 compared to the rest of the study reach

Year interval	Subreach 19			Remainder of study reach		
	Channel length with lateral activity[a] (ft)	Mean migration rate over active sections[a] (ft yr^{-1})	Mean migration rate over reach[b] (ft yr^{-1})	Channel length with lateral activity[a] (ft)	Mean migration rate over active sections[a] (ft yr^{-1})	Mean migration rate over reach[b] (ft yr^{-1})
1951-2010	1298	0.19 ± 0.06	0.031	7641	0.21 ± 0.03	0.094
1951-1959	450	0.41 ± 0.26	0.023	4959	0.77 ± 0.12	0.23
1959-1966	12	0.06 ± 0.01	0	2731	1.48 ± 0.34	0.12
1966-1979	3711	0.70 ± 0.11	0.33	6443	0.61 ± 0.10	0.12
1979-1987	4037	0.79 ± 0.15	0.40	3373	0.70 ± 0.14	0.073
1987-1995	606	0.59 ± 0.14	0.045	5938	0.75 ± 0.15	0.14
1995-2010	326	0.67 ± 0.06	0.027	5964	0.63 ± 0.19	0.12

a Exceeding error margin
b Calculated as a weighted mean of active and non-active reach lengths

6 Conclusion

Based on the field inventory, the loading of large woody debris is 16.6 pieces/100 m or 3.4 m^3/100 m over the majority of the study reach located in the lower San Antonio River. When the reach upstream of Elm Bayou is included the loading increases by an order of magnitude. These loadings are relatively low compared to known loadings in other rivers but exceed that found in the nearby Sabine River. The variability in the spatial distribution of the LWD suggests that future inventories should be based on frequent spatial sampling of the overall reach of interest that meets or exceeds the strategy outlined herein. Further, any attempt to explore how channel morphology may affect where LWD is deposited requires a stratified sampling strategy that captures key aspects of river morphology (e.g., bend apices).

Based on LWD characteristics and their relation to channel characteristics, the woody debris appears to be quite mobile during floods. In fact, the estimated LWD delivery rate of about 30,000 ft^3yr^{-1} suggests that pieces are easily transported until trapped within the reach upstream of the Elm Bayou confluence. Evidence from aerial photography suggests that the accumulation of LWD in this subreach will persist into the future given the same wood budget dynamics in the watershed.

The accumulation of LWD near Elm Bayou has the potential to change the frequency of overbank flooding based on an initial order of magnitude analysis. With a very large volume of tightly packed wood, bankfull conditions might be exceeded around 6% of the time, which is an order of magnitude increase from current conditions. Further analysis should be conducted to refine these first approximation results by taking into account other factors that could affect the discharge at bankfull conditions, such as the resistance offered by the woody debris.

Overall the study reach exhibits a low rate of lateral migration, which is limited to a small portion of the channel. Based on the analysis, the reach upstream of Elm Bayou is less active

overall than the other part of the study reach. Nonetheless, persistence of LWD coupled with an increased volume of tightly packed wood does have the potential to influence channel position in the future.

7 References cited

Benda, L.E., Bigelow, P.E. and Worsley, T.M., 2002. Recruitment of wood to streams in old-growth and second-growth redwood forests, northern California, U.S.A. Canadian Journal of Forest Research, 32: 1460-1477.

Bilby, R.E. and Ward, J.W., 1989. Changes in characteristics and function of woody debris with increasing size of streams in Western Washington. Transactions of the American Fisheries Society, 118: 368-378.

Braudrick, C.A., Grant, G.E., Ishikawa, Y. and Ikeda, H., 1997. Dynamics of wood transport in streams: a flume experiment. Earth Surface Processes and Landforms, 22: 669-683.

Gurnell, A.M., 1997. Channel change on the River Dee meanders, 1946-1992, from the analysis of air photographs. Regulated Rivers: Research & Management, 13: 13-26.

Hassan, M.A. et al., 2005. Spatial and temporal dynamics of wood in headwater streams of the Pacific Northwest. Journal of the American Water Resources Association, 41(4): 899-919.

Hogan, D.L., 1987. The influence of large organic debris on channel recovery in the Queen Charlotte Islands, British Columbia, Canada, Erosion and Sedimentation in the Pacific Rim. IAHS publ. no 165, pp. 343-353.

Hyatt, T.L. and Naiman, R.J., 2001. The residence time of large woody debris in the Queets River, Washington, USA. Ecological Applications, 11(1): 191-202.

Keller, E.A. and Swanson, F.J., 1979. Effects of large organic material on channel form and fluvial processes. Earth Surface Processes, 4: 361-380.

Lemly, A.D. and Hilderbrand, R.H., 2000. Influence of large woody debris on stream insect communities and benthic detritus. Hydrobiologia, 421: 179-185.

Lienkaemper, G.W. and Swanson, F.J., 1987. Dynamics of large woody debris in streams in old-growth douglas-fir forests. Canadian Journal of Forest Research, 17(2): 150-156.

Manga, M. and Kirchner, J.W., 2000. Stress partitioning in streams by large woody debris. Water Resources Research, 36(8): 2373-2379.

McBroom, M.W., 2010. Developing large woody debris budgets for Texas rivers. Texas Water Development Board Report 0604830632, 146 pp.

Micheli, E.R. and Kirchner, J.W., 2002. Effects of wet meadows riparian vegetation on streambank erosion. 1. remote sensing measurement of streambank migration and erodibility. Earth Surface Processes and Landforms, 27: 627-639.

Montgomery, D.R. et al., 1996. Distribution of bedrock and alluvial channels in forested mountain drainage basins. Nature, 381(13): 587-589.

Mount, N.J., Louis, J., Teeuw, R.M., Zukowshyj, P.M. and Stott, T., 2003. Estimation of error in bankfull width comparisons from temporally sequenced raw and corrected aerial photographs. Geomorphology, 56: 1-13.

Rhoades, E.L., O'Neal, M.A. and Pizzuto, J.E., 2009. Quantifying bank erosion on the South River from 1937 to 2005, and its importance in assessing Hg contamination. Applied Geography, 29: 125-134.

Tiegs, S.D. and Pohl, M., 2005. Planform channel dynamics of hte lower Colorado River: 1976-2000. Geomorphology, 69: 14-27.
Wohl, E. et al., 2010. Large in-stream wood studies: a call for common metrics. Earth Surface Processes and Landforms, 35: 618-625.
Yao, Z., Ta, W., Jia, X. and Xiao, J., 2011. Bank erosion and accretion along the Ningxia-Inner Mongolia reaches of the Yellow River from 1958 to 2008. Geomorphology, 127: 99-105.